Title

In Vivo Single-Cell Detection of Metabolic Oscillations in Stem Cells

Journal

Cell Reports, 10(1)

ISSN

2639-1856

Authors

Stringari, Chiara
Wang, Hong
Geyfman, Mikhail
et al.

Publication Date

2015

DOI

10.1016/j.celrep.2014.12.007

Peer reviewed

Published in final edited form as:
Cell Rep. 2015 January 6; 10(1): 1–7. doi:10.1016/j.celrep.2014.12.007.

In vivo single cell detection of metabolic oscillations in stem cells

Chiara Stringari[1,2], **Hong Wang**[3,4], **Mikhail Geyfman**[3], **Viera Crosignani**[1], **Vivek Kumar**[5,6], **Joseph S. Takahashi**[5,6], **Bogi Andersen**[3,7,8,9,*], and **Enrico Gratton**[1,8,*]

[1]Laboratory of Fluorescence Dynamics, Biomedical Engineering Department, University of California, Irvine, CA 92037, USA

[2]Laboratory for Optics and Biosciences, École Polytechnique, 91128 Palaiseau Cedex, France

[3]Department of Biological Chemistry, School of Medicine, University of California, Irvine, CA 92037, USA

[4]State Key Laboratory for Agrobiotechnology, College of Biological Sciences, China Agricultural University, Beijing 100083, China

[5]Department of Neuroscience, University of Texas Southwestern Medical Center, Dallas, TX 75390, USA

[6]Howard Hughes Medical Institute, University of Texas Southwestern Medical Center, Dallas, TX 75390, USA

[7]Department of Medicine, School of Medicine, University of California, Irvine, CA 92037, USA

[8]Center for Complex Biological System, University of California, Irvine, CA 92037, USA

[9]Institute for Genomics and Bioinformatics, University of California, Irvine, CA 92037, USA

Summary

Using bulk measurements in metabolic organs, the circadian clock was shown to play roles in organismal energy homeostasis. However, the relationship between metabolic and circadian oscillations has not been studied *in vivo* at a single cell level. Also, it is unknown whether the circadian clock controls metabolism in stem cells. We used a sensitive, non-invasive method to detect metabolic oscillations and circadian phase within epidermal stem cells in live mice at the single cell level. We observe a higher NADH/NAD+ ratio, reflecting an increased glycolysis/oxidative phosphorylation ratio, during the night compared to the day. Furthermore, we

*Co-senior authors to whom correspondence should be addressed to: Bogi Andersen, bogi@uci.edu, Enrico Gratton, egratton@uci.edu.

Author Contributions:
CS, MG, VK, JST, BA and EG conceived of and designed the experiments, and analyzed the data. CS, HW, MG and VC performed the experiments. CS, BA and EG wrote the manuscript with input from all other authors.

The authors have no financial conflict of interest to declare.

demonstrate that single cell metabolic heterogeneity within the basal cell layer correlates with the circadian clock and that diurnal fluctuations in NADH/NAD+ ratio are *Bmal1* dependent. Our data show that in proliferating stem cells the circadian clock coordinates activities of oxidative phosphorylation and glycolysis with DNA synthesis, perhaps as a protective mechanism against genotoxicity.

Introduction

The circadian clock is a self-sustained cellular oscillator that coordinates appropriate metabolic responses within peripheral tissues with the light/dark cycle. Recent studies demonstrated that the circadian clock and metabolism are tightly interconnected (Bass, 2010; Eckel-Mahan, 2013; Sahar, 2009). Thus, circadian clock-regulated transcription feedback loops in the liver produce cycles of NAD+ biosynthesis, ATP production and mitochondrial respiration, and conversely the cellular redox status influences the activity of clock transcription factors (Peek, 2013). So far, *in vivo* evaluations of metabolic oscillations have been done through bulk tissue experiments. Furthermore, it remains unknown whether the circadian clock is involved in metabolism control in stem cells that maintain self-renewing epithelia.

The interfollicular epidermis, a prototype proliferative epithelium, contains a basal cell layer where the majority of cells are highly proliferative stem or progenitor cells that exit the cell cycle as they move into the suprabasal compartment for differentiation and formation of a protective barrier (Clayton, 2007; Lim, 2013; Mascre, 2012). Studies in a number of different mammals demonstrated a striking time-of-day dependent variation in stem cell proliferation in the epidermis (Bjarnason and Jordan, 2002; Brown, 1991) and other proliferative epithelia such as the intestine (Potten et al., 1977). More recent studies have started to cast light on how the time-of-day dependent variation in cell proliferation is regulated, showing that core circadian clock components are required for this feature (Gaddameedhi et al., 2011; Geyfman et al., 2012; Janich et al., 2011; Janich et al., 2013; Plikus et al., 2013).

The biological function of time-of-day dependent stem cell proliferation remains unexplained (Gaddameedhi, 2011; Geyfman, 2012; Janich, 2013; Plikus, 2013). One hypothesis is that organisms have evolved to temporally separate DNA synthesis from metabolic functions such as oxidative phosphorylation as a protective mechanism, as has been suggested for metabolic cycles in yeast (Tu, 2005). Energy production through oxidative phosphorylation creates high levels of ROS, which damage DNA leading to cellular toxicity, cancer and aging. A previous study reported that the expression of genes involved in oxidative phosphorylation and the skin's ROS levels are BMAL1 dependent and antiphasic to the peak in S-phase for stem cells (Geyfman, 2012). The limitation of these studies is that, except for the quantitation of cell proliferation, they are based on measurements in the cellularily complex skin and rely on inference from gene expression rather than direct measurements of metabolites.

In order to study metabolism of stem cells of the epidermal basal cell layer *in vivo*, we applied Two-Photon Excitation (TPE) and Fluorescence Lifetime Imaging microscopy

(FLIM) of the intrinsic metabolic biomarker NADH (Heikal, 2010; Koenig, 2003; Stringari, 2011) (Fig. 1). This optical method is non-invasive and provides sensitive and quantitative measurement of free and protein-bounds NADH levels, which reflect the metabolic state of single cells within the native microenvironment of the living tissue (Stringari, 2011; Stringari, 2012a). The free and bound NADH ratio reflects the NADH/NAD+ redox ratio (Bird, 2005; Skala, 2007), an indicator of the relative level of glycolysis and oxidative phosphorylation within the cell (Bird, 2005; Stringari, 2012a) (See Supplemental Information).

Results

We first performed *in vivo* imaging of NADH auto fluorescence and collagen second harmonic generation (SHG) in adult mouse skin (Fig. 1A,B,C) to determine whether we could utilize the SHG from the dermis to localize cells of the basal cell layer. This approach was successful as NADH is excited at 740nm within cells of the epidermal basal cell layer, located right above the collagen fibers of the dermis (Fig. 1C and S1). The two-photon fluorescence intensity NADH distribution highlights single cell morphology with relatively dim nuclei and bright mitochondria (Fig. 1C,E and Fig. 2A). Analysis of the FLIM images is performed by a Fast Fourier transform (FFT) of the FLIM raw data (Fig. 1D,E), by creating a 2D histogram (phasor plot) of the NADH FLIM image where every pixel of the FLIM image is transformed into a pixel in the phasor plot (Fig. 2A,B). The phasor coordinates g (x) and s (y) are the real and the imaginary part of the FFT transformation (Supplemental Information), respectively, and the g coordinate is the most sensitive to free/bound NADH variations (Stringari, 2011; Stringari, 2012a). The broad NADH lifetime distribution (Fig. 1D and Fig. 2B) has a characteristic linear-elongated pattern that reflects a mixture of free and bound NADH, yielding information on different distributions of metabolic states and redox ratios of the cells over the time (Stringari, 2012a).

We next used fluorescence lifetime measurement of intrinsic NADH within single cells (Fig. 1D,E) of the basal cell layer to determine whether there are time of day dependent fluctuations in NADH levels (Fig. 2). We found that metabolic oscillations in the NADH cellular fingerprints follow a diurnal pattern, showing a consistent variation in free/bound NADH ratios between day and night (Fig. 2 and S2). Mapping the relative concentration of free (purple) and bound (cyan) NADH within cells of the basal cell layer at different time points of the day, according to the FLIM phasor location of the free NADH and the bound NADH measured in solution (Stringari, 2011), we found greater free to bound NADH ratios at 2AM and 8AM than 2PM and 8PM (Fig. 2A,B). In these studies, the metabolic optical fingerprint of single stem cells is measured through the average phasor FLIM value of the entire cell, including cytoplasmic, mitochondrial and nuclear NADH (Fig. 1E). Mitochondrial NADH is the major contributor to the cellular metabolic optical fingerprint since mitochondria are brighter than cytoplasm and nucleus and occupy a higher percentage of the cell volume (Fig. 1D). For quantification, the cellular phasor values were then plotted in the scatter diagram, showing that the average FLIM phasor values of basal cells are significantly different according to the hours of the day, indicating a different metabolic state (t-test between the g coordinate of single cells, $p<0.0001$, Fig. 2B). We found consistent results in six independent measurements (Fig. S2). The relative concentration of

free/bound NADH within stem cells are highest during the night at 2AM and 8AM, decreasing significantly during the day at 2PM and 8PM (Fig. 2B,C). The histogram of the g coordinate of the cell phasor fingerprints (which is proportional to the free/bound NADH ratio) displays a circadian metabolic oscillation with a peak at 2AM in phase with the highest percentage of cells in S phase (Fig. 2C).

Different ratios of free and protein-bound NADH reflect different redox ratios (NADH/NAD+) which in turn reflect the relative rates of glycolysis and oxidative phosphorylation (Glycolysis/OXPHOS ratio) (Bird, 2005; Stringari, 2012a) (See Supplemental Information). The time of day dependent free/bound NADH oscillations suggest that cells of the basal cell layer have relatively higher rate of glycolysis during the night while during the day they present relatively higher rates of oxidative phosphorylation. The glycolytic and the oxidative phosphorylation phenotypes measured during the night and day (Fig. 2), respectively, correlate with previously described time-of-day variation in S-phase in epidermal stem cells with the high OXPHOS state being antiphasic to maximum S-phase (Fig. 2C) (Geyfman, 2012). The metabolic oscillations that we measure *in vivo* in basal cell layer stem cells are also consistent with the NAD+ circadian rhythmicity and the mitochondrial oxidative respiration rates recently measured in liver cells (Peek, 2013).

The phasor FLIM analysis at single cell resolution reveals significant cell-to-cell heterogeneity in the metabolic signature as indicated by the intrinsic free and protein-bound NADH concentrations (Fig. 1D,E and Fig. 2B). To quantify the inter-cell metabolic heterogeneity within the basal cell layer, we determined the standard deviation of the phasor coordinates g over the entire population of recorded cells. The measured standard deviation of the g cell phasor coordinates has a typical value between 0.008 and 0.034 (Fig. 2B and S2), which is significantly larger than the experimental error on a single cell phasor measurement (0.002 with the Signal-to-Noise ratio of the experiment (Stringari, 2012b)). Hence the free/bound NADH distribution we observe reflects a biological variation and true heterogeneity of the cellular metabolic fingerprint within the population of basal cells.

To investigate whether there is a correlation between the metabolic fingerprint and the circadian phase we performed NADH FLIM measurements on the epidermis of Per1-Venus mice expressing the fluorescent protein VENUS from the clock-controlled Per1 promoter (Cheng, 2009). The circadian clock phase of individual progenitors of the basal cell layer was evaluated by exciting the tissue at 940nm wavelength and measuring the intensity of the Per1-Venus reporter (see Experimental Procedures; Fig. S3). As reported before (Cheng, 2009), the average intensity of the Per1-Venus reporter is higher at 2AM and 8AM than 2PM and 8PM (Fig. 3A,B). The phase of the Per1-Venus clock reporter correlates with high ratios of free to bound NADH and glycolysis/OXPHOS ratios (i.e. high values of g coordinate of single cell phasor fingerprints). Furthermore, we found a linear correlation between the cellular metabolic fingerprint (g coordinate of single cell phasor) and the circadian-clock phase of individual cells (Per1-Venus reporter intensity) (Fig. 3C). Thus, the circadian clock output and the redox state show significant cell-to-cell heterogeneity and are tightly correlated at a cellular level.

To determine whether the daily fluctuations of NADH in progenitor cells of the basal cell layer are controlled by the circadian clock, we evaluated the metabolic fingerprint of epidermal stem cells in *Bmal1*−/− mice, which lack circadian rhythm (Bunger, 2000). We found that time-of-day dependent metabolic oscillations of the progenitor cells in the epidermal basal cell layer are obliterated in the *Bmal1*−/− mice, (in Fig. 4 the difference between the *Bmal1*−/− cell fingerprints at 2 AM and 2PM is not statistically significant (t-test p=0.37)); these results were consistently observed in three independent measurements (Fig. S4). As the *Bmal1*−/− mice were kept under normal 12:12 LD conditions during which the animals are entrained as measured by wheel running, these experiments show that BMAL1 is required for diurnal variation in the free to bound ratio of NADH in stem cells of the interfollicular epidermis.

Discussion

Previous studies have shown that proliferation of interfollicular epidermal stem cells is highly diurnal, with a greater percentage of cells undergoing S-phase during the night than during the day in mice, and that this diurnal variation in cell proliferation depends on the core circadian clock gene *Bmal1* acting within keratinocytes (Gaddameedhi, 2011; Geyfman, 2012; Plikus, 2013). While there is controversy about the hierarchy of cells within the basal layer of the interfollicular epidermis, previous work generally supports the idea that during normal homeostasis the mouse epidermis is primarily maintained by a single type of progenitor/stem cell (Clayton, 2007; Lim, 2013; Mascre, 2012). In this study we have used FLIM, a label-free, single-cell resolution technique that detects the levels of bound and free NADH *in vivo*, to identify diurnal metabolic oscillations in stem cells of the interfollicular epidermis. The implementation of FLIM overcomes limitations of previous studies into the role of the circadian clock in metabolism based on bulk measurements, allowing the detection of metabolic heterogeneity within stem cells of the epidermis and correlation of this heterogeneity to clock output at a single cell level.

Our study supports the idea that the circadian clock regulates metabolism within stem cells of the interfollicular epidermis for the following reasons. *First*, we find a correlation between the NADH/NAD+ redox ratio as measured by FLIM and clock output as measured by activity of the Per1-Venus reporter *in vivo*. *Second*, we find that mutations in *Bmal1* disrupt the diurnal variation in the NADH/NAD+ redox ratio. Through regulation of gene expression within metabolic organs, the circadian clock has been shown to play a key role in diurnal shifts in organismal metabolic patterns (Peek, 2013; Sahar, 2009). Our study indicates that the circadian clock also has a key function in the modulation of metabolism within stem cells of a highly proliferative epithelial tissue. We show significant cell to cell heterogeneity in circadian output and NADH/NAD+ redox ratios, perhaps reflecting different levels of stemness among the epidermal basal cells.

Interestingly, we find that the epidermal stem cells show a more glycolytic phenotype during night when the highest numbers of cells are in S-phase (Geyfman, 2012). It has long been observed that proliferating cells rely more on glycolysis than oxidative phosphorylation, such as in the Warburg effect in cancer cells (Warburg, 1956). Reactive oxygen species (ROS) are a normal mitochondrial byproduct of oxidative phosphorylation during cellular

respiration (Murphy, 2009). While also serving normal signaling roles (D'Autreaux and Toledano, 2007), ROS is toxic to the cell, oxidizing a variety of macromolecules including DNA where it causes mutations. Thus, the accumulation of ROS-mediated cellular damage is thought to play a role in carcinogenesis and aging. All tissues are susceptible to ROS-induced DNA damage, but since the S-phase of the cell cycle is the most susceptible cellular stage, highly proliferative tissues are likely most sensitive to ROS-induced mutagenesis, thus providing one possible explanation for proliferating cells' reliance on glycolysis (Hamanaka, 2011). Our findings suggest that the circadian clock confers time-of-day dependent shifts in glycolysis versus oxidative phosphorylation within proliferating epithelial stem cells, thus minimizing DNA damage during S-phase. Conversely, in BMAL mutant mice, which show no temporal separation of glycolytic and oxidative metabolism, this protection is presumably lost, leading to increased DNA damage. Indeed, mutations in *Bmal1* have been associated with premature aging and increased DNA damage (Janich, 2011; Kondratov RV1, 2006).

Experimental Procedures

Animal models and procedures

Mice were kept under 12h:12h LD cycle (Light on at 6:30AM) with unrestricted access to food and water. Immediately before imaging, mice were anesthetized with ketamine. Hair was shaved and removed with NAIR® hair remover (Church & Dwight Co., Inc) on the back in a 2 cm^2 area, which was washed under warm water and dried with Kimwipes®. Procedures were approved by the Institutional Animal Care and Use Committee (protocols 2002–2357-3 and 2001–2239). *Bmal1*−/− and Per1-Venus mice were previously described (Bunger, 2000; Cheng, 2009). *Bmal1*−/− mice and controls were studied during first telogen at ages 20 to 22 days.

Imaging

Imaging was performed with a Zeiss 710 microscope coupled to a Ti:Sapphire laser system (Spectra-Physics Mai Tai). A 40 × 0.8 NA water immersion objective (LUMPlanFl Olympus) with 2mm working distance was used. The excitation wavelengths were 880nm and 740 nm with average power of about 5 mW. Fluorescence intensity images of NADH were acquired by exciting the tissue at 740 nm and placing a 460/80 nm emission filter in front of the detector. Second Harmonic Generation from collagen was excited at 880nm and collected with an emission filter 440/20nm or excited at 940nm and collected with a band pass filter 470/20nm. The stem cells within the epidermal basal cell layer are identified by their unique location immediately above the collagen layer of the dermis; a Second Harmonic Generation 3D stack was systematically acquired to localize the edge of the dermis layer in the Z axis (Fig. S1). For example in Fig. S1C, the edge of the dermis is identified at a depth of 18μm corresponding to the last Z-section of the dermis that contains collagen. To localize the epidermal basal layer, we moved the focus in Z between 2 and 4 μm above the edge of the dermis layer. (In figure Fig. S1B, the epidermal basal layer is located between 14 and 16 μm). The epidermal basal layer is characterized (Fig. S1B) by small and round shaped stem cells, while cells that undergo differentiation in the upper

layers are larger. Six regions of interest of the epidermal basal layer were imaged within the $2cm^2$ skin. We imaged four mice for every time point and condition.

Fluorescence lifetime images were acquired with a ISS A320 FastFLIM system (Colyer, 2008). For image acquisition the following settings are used: image size of 256 × 256 pixels and scan speed of 25 usec/pixel. A dichroic filter (690 nm) was used to separate the fluorescence signal from the laser light and the fluorescence. For the acquisition of FLIM images, fluorescence is detected by a photomultiplier (H7422P-40 of Hamamatsu) and a 610 nm short pass filter is placed in front of the detector. A 495nm long pass filter separates the blue and the green fluorescence. NADH fluorescence was collected through a 460/80 nm filter. FLIM data are acquired and processed by the SimFCS software developed at the Laboratory of Fluorescence Dynamics. FLIM calibration of the system is performed by measuring the known lifetime of the fluorescein with a single exponential of 4.04 ns. FLIM data are collected until 100 counts in the brightest pixel of the image are acquired. Typically the acquisition time was of the order of few seconds. To quantify Per1-Venus intensity we excited the epidermal basal layer with a wavelength of 940nm, acquiring 10 frames for each field of view (Fig. S3C). The same laser power of 5mW was used for all fields of view. We verified that the Venus fluorescence signal of cells was not affected by photobleaching or photodamage by scanning 20 frames on the same field of view (Fig. S3C).

FLIM Phasor data analysis

Every pixel of the FLIM image is transformed in one pixel in the 2-dimentional histogram of the phasor plot through a mathematical transformation of the fluorescence intensity decay that involves Fast Fourier Transformation (FFT) ((Digman, 2008; Stringari, 2011) and Supplemental Information). The coordinates g and s (x and y coordinates respectively) in the phasor plot are the real and imaginary part of the FFT. The analysis of the phasor distribution is performed by cluster identification of free and bound NADH. Because of the linearity of the phasor coordinates, mixtures of free and bound NADH in the focal volume will distribute along the line that connects the pure molecular species. Fractional intensities of chemical species in every pixel of the image were evaluated with a graphical analysis in the phasor plot as described previously (Digman, 2008; Stringari, 2011). We performed image segmentation on the FLIM data by selecting the region of interest of cells within the tissue, using a cursor with circular shape. We then calculated the phasor average value within the entire cell, including NADH in mitochondria and nuclei. When measuring the cell phasor, all pixels of the cell (about 1000) are taken in account and the signal to noise ratio of the FLIM signature of cells is higher than in single pixels. The average value of the standard deviation of the NADH average cell phasor is calculated over the 5 different independent experiments in Figure 2 and S2.

Supplementary Material

Refer to Web version on PubMed Central for supplementary material.

Acknowledgments

Work supported with NIH grants R01 AR056439, P50 GM076516 and P41 GM103540.

References

Bass J, Takahashi JS. Circadian integration of metabolism and energetics. Science. 2010; 330:1349–1354. [PubMed: 21127246]

Bird DK, Yan L, Vrotsos KM, Eliceiri KW, Vaughan EM, Keely PJ, White JG, Ramanujam N. Metabolic mapping of MCF10A human breast cells via multiphoton fluorescence lifetime imaging of the coenzyme NADH. Cancer Res. 2005; 65:8766–8773. [PubMed: 16204046]

Bjarnason GA, Jordan R. Rhythms in human gastrointestinal mucosa and skin. Chronobiol Int. 2002; 19:129–140. [PubMed: 11962671]

Brown WR. A review and mathematical analysis of circadian rhythms in cell proliferation in mouse, rat, human epidermis. J Invest Dermatol. 1991; 97:273–280. [PubMed: 1830075]

Bunger M, Wilsbacher LD, Moran SM, Clendenin C, Radcliffe LA, Hogenesch JB, Simon MC, Takahashi JS, Bradfield CA. Mop3 is an essential component of the master circadian pacemaker in mammals. Cell. 2000; 103:1009–1017. [PubMed: 11163178]

Cheng H, Alvarez-Saavedra M, Dziema H, Choi YS, Li A, Obrietan K. Segregation of expression of mPeriod gene homologs in neurons and glia: possible divergent roles of mPeriod1 and mPeriod2 in the brain. Hum Mol Genet. 2009; 18:3110–3124. [PubMed: 19477955]

Clayton E, Doupe DP, Klein AM, Winton DJ, Simons BD, Jones PH. A single type of progenitor cell maintains normal epidermis. Nature. 2007; 446:185–189. [PubMed: 17330052]

Colyer R, Lee C, Gratton E. A novel fluorescence lifetime imaging system that optimizes photon efficiency. Microsc Res Tech. 2008; 71:201–213. [PubMed: 18008362]

D'Autreaux B, Toledano MB. ROS as signalling molecules: mechanisms that generate specificity in ROS homeostasis. Nat Rev Mol Cell Biol. 2007; 8:813–824. [PubMed: 17848967]

Digman M, Caiolfa VR, Zamai M, Gratton E. The phasor approach to fluorescence lifetime imaging analysis. Biophys J. 2008; 94:L14–L16. [PubMed: 17981902]

Eckel-Mahan K, Sassone-Corsi P. Metabolism and the circadian clock converge. Physiol Rev. 2013; 93:107–135. [PubMed: 23303907]

Gaddameedhi S, Selby CP, Kaufmann WK, Smart RC, Sancar A. Control of skin cancer by the circadian rhythm. Proc Natl Acad Sci U S A. 2011; 108:18790–18795. [PubMed: 22025708]

Gaddameedhi S, Selby CP, Kaufmann WK, Smart RC, Sancar A. Control of skin cancer by the circadian rhythm. Proc Natl Acad Sci. 2011; 108:18790–18795. [PubMed: 22025708]

Geyfman M, Kumar V, Liu Q, Ruiz R, Gordon W, Espitia F, Cam E, Millar SE, Smyth P, Ihler A, et al. Brain and muscle Arnt-like protein-1 (BMAL1) controls circadian cell proliferation and susceptibility to UVB-induced DNA damage in the epidermis. Proc Natl Acad Sci U S A. 2012; 109:11758–11763. [PubMed: 22753467]

Geyfman M, Kumar V, Liu Q, Ruiz R, Gordon W, Espitia F, Cam E, Millar SE, Smyth P, Ihler A, Takahashi JS, Andersen B. Brain and muscle Arnt-like protein-1 (BMAL1) controls circadian cell proliferation and susceptibility to UVB-induced DNA damage in the epidermis. Proc Natl Acad Sci U S A. 2012; 109:11758–11763. [PubMed: 22753467]

Hamanaka R, Chandel NS. Cell biology. Warburg effect and redox balance. Science. 2011; 334:1219–1220. [PubMed: 22144609]

Heikal AA. Intracellular coenzymes as natural biomarkers for metabolic activities and mitochondrial anomalies. Biomark Med. 2010; 4:241–263. [PubMed: 20406068]

Janich P, Pascual G, Merlos-Suarez A, Batlle E, Ripperger J, Albrecht U, Cheng HY, Obrietan K, Di Croce L, Benitah SA. The circadian molecular clock creates epidermal stem cell heterogeneity. Nature. 2011; 480:209–214. [PubMed: 22080954]

Janich P, Pascual G, Merlos-Suárez A, Batlle E, Ripperger J, Albrecht U, Cheng HY, Obrietan K, Di Croce L, Benitah SA. The circadian molecular clock creates epidermal stem cell heterogeneity. Nature. 2011; 480:209–214. [PubMed: 22080954]

Janich P, Toufighi K, Solanas G, Luis NM, Minkwitz S, Serrano L, Lehner B, Benitah SA. Human epidermal stem cell function is regulated by circadian oscillations. Cell stem cell. 2013; 13:745–753. [PubMed: 24120744]

Janich P, Toufighi K, Solanas G, Luis NM, Minkwitz S, Serrano L, Lehner B, Benitah SA. Human Epidermal Stem Cell Function Is Regulated by Circadian Oscillations. Cell Stem Cell. 2013; 13:745–753. [PubMed: 24120744]

Koenig K, Riemann I. High-resolution multiphoton tomography of human skin with subcellular spatial resolution and picosecond time resolution. J Biomed Opt. 2003; 432

Kondratov RV1 KA, Gorbacheva VY, Vykhovanets OV, Antoch MP. Early aging and age-related pathologies in mice deficient in BMAL1, the core component of the circadian clock. Genes Dev. 2006; 20:1868–1873. [PubMed: 16847346]

Lim X, Tan SH, Koh WL, Chau RM, Yan KS, Kuo CJ, van Amerongen R, Klein AM, Nusse R. Interfollicular epidermal stem cells self-renew via autocrine Wnt signaling. Science. 2013; 342:1226–1230. [PubMed: 24311688]

Mascre G, Dekoninck S, Drogat B, Youssef KK, Brohee S, Sotiropoulou PA, Simons BD, Blanpain C. Distinct contribution of stem and progenitor cells to epidermal maintenance. Nature. 2012; 489:257–262. [PubMed: 22940863]

Murphy MP. How mitochondria produce reactive oxygen species. Biochem J. 2009; 417:1–13. [PubMed: 19061483]

Peek C, Affinati AH, Ramsey KM, Kuo HY, Yu W, Sena LA, Ilkayeva O, Marcheva B, Kobayashi Y, Omura C, Levine DC, Bacsik DJ, Gius D, Newgard CB, Goetzman E, Chandel NS, Denu JM, Mrksich M, Bass J. Circadian clock NAD+ cycle drives mitochondrial oxidative metabolism in mice. Science. 2013; 342:1243417. [PubMed: 24051248]

Plikus M, Vollmers C, de la Cruz D, Chaix A, Ramos R, Panda S, Chuong CM. Local circadian clock gates cell cycle progression of transient amplifying cells during regenerative hair cycling. Proc Natl Acad Sci. 2013; 110:E2106–E2115. [PubMed: 23690597]

Plikus MV, Vollmers C, de la Cruz D, Chaix A, Ramos R, Panda S, Chuong CM. Local circadian clock gates cell cycle progression of transient amplifying cells during regenerative hair cycling. Proc Natl Acad Sci U S A. 2013; 110:E2106–E2115. [PubMed: 23690597]

Potten CS, Al-Barwari SE, Hume WJ, Searle J. Circadian rhythms of presumptive stem cells in three different epithelia of the mouse. Cell Tissue Kinet. 1977; 10:557–568. [PubMed: 922804]

Sahar S, Sassone-Corsi P. Metabolism and cancer: the circadian clock connection. Nat Rev Cancer. 2009; 9:886–896. [PubMed: 19935677]

Skala MC, Riching KM, Gendron-Fitzpatrick A, Eickhoff J, Eliceiri KW, White JG, Ramanujam N. In vivo multiphoton microscopy of NADH and FAD redox states, fluorescence lifetimes, and cellular morphology in precancerous epithelia. Proc Natl Acad Sci U S A. 2007; 104:19494–19499. [PubMed: 18042710]

Stringari C, Cinquin A, Cinquin O, Digman MA, Donovan PJ, Gratton E. Phasor approach to fluorescence lifetime microscopy distinguishes different metabolic states of germ cells in a live tissue. Proc Natl Acad Sci U S A. 2011; 108:13582–13587. [PubMed: 21808026]

Stringari C, Edwards RA, Pate KT, Waterman ML, Donovan PJ, Gratton E. Metabolic trajectory of cellular differentiation in small intestine by Phasor Fluorescence Lifetime Microscopy of NADH. Sci Rep. 2012a; 2

Stringari C, Nourse JL, Flanagan L, Gratton E. Phasor Fluorescence Lifetime Microscopy of free and protein-bound NADH reveals neural Stem Cell Differentiation Potential, PLoS One. 2012b; 7:e48014. [PubMed: 23144844]

Tu B, Kudlicki A, Rowicka M, McKnight SL. Logic of the yeast metabolic cycle: temporal compartmentalization of cellular processes. Science. 2005; 310:1152–1158. [PubMed: 16254148]

Warburg O. On the origin of cancer cells. Science. 1956; 123:309–314. [PubMed: 13298683]

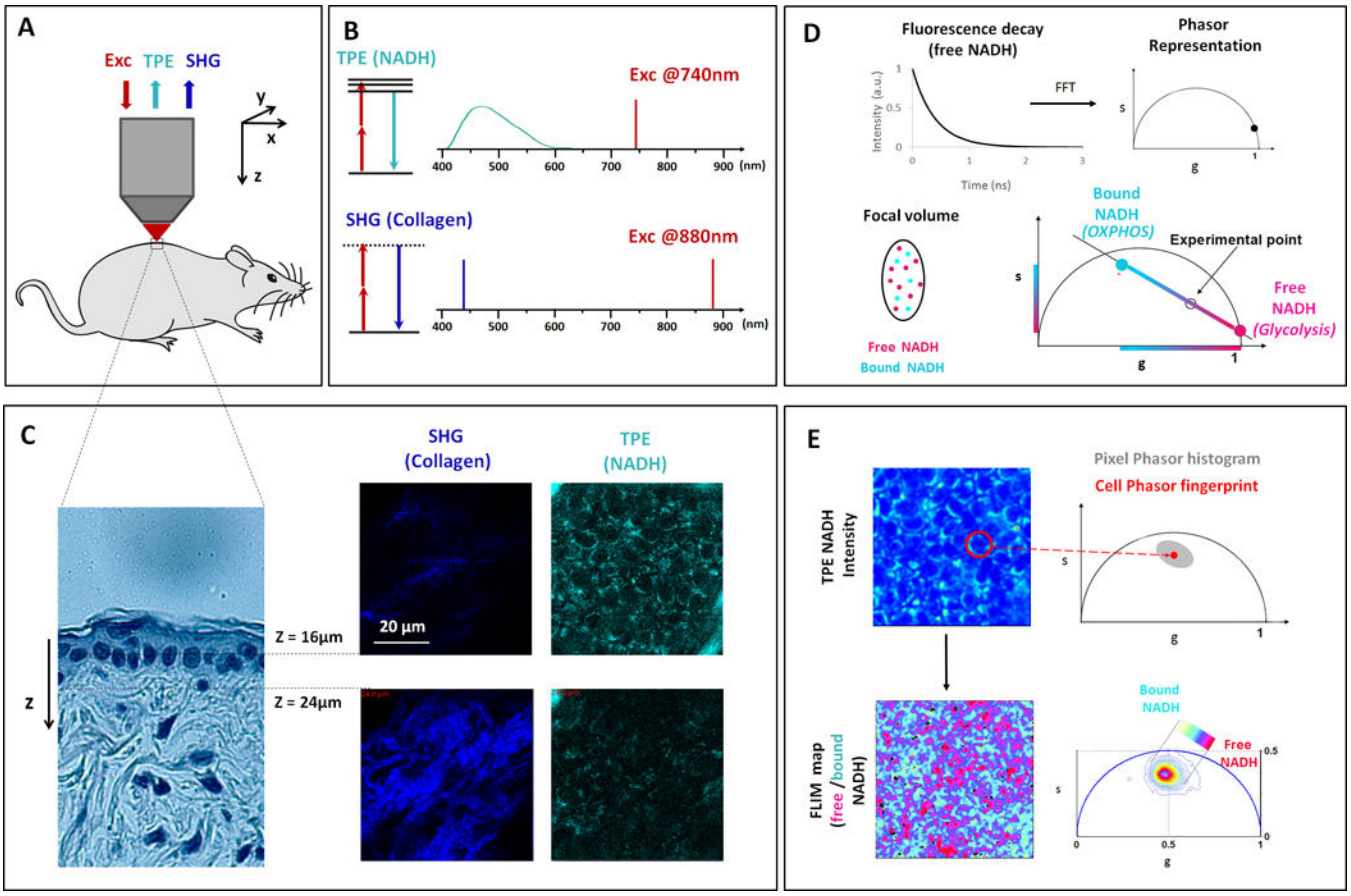

Figure 1. ***In vivo*** **non-invasive NADH imaging of stem cells within the epidermal basal cell layer**

(A) Scheme of the live mouse imaging. Two-Photon Excitation fluorescence (TPE) from NADH (cyan) and Second Harmonic Generation (SHG) from collagen are collected in epidetection through the same objective of the Excitation (Exc), represented in red. **(B)** Energy diagrams and wavelengths involved in the TPE and SHG. **(C)** A representative cross section of mouse skin showing the epidermis separated from the dermis by a basal lamina. Second Harmonic Generation (SHG) signal from dermal collagen fibers is excited at 880nm and collected with a 440/20nm filter. NADH TPE fluorescence intensity is excited at 740nm and collected with a 460/80 nm filter highlighting single stem cells within the basal layer. **(D)** After a mathematical transformation that involves Fast Fourier Transformation (FFT) (Material and Methods and (Digman, 2008)), the measured Fluorescence Lifetime decay is represented by a single point in the 2D phasor plot with g and s coordinates corresponding to the real and imaginary part of the FFT. Because of the linearity of the phasor coordinates, mixtures of free and bound NADH in the focal volume will lay along the line that connects the pure molecular species (Stringari, 2011). **(E)** Phasor analysis of the FLIM images is performed both at the pixel level and cell level. Single pixels are painted in the FLIM map according to a linear cursor (from purple to cyan) that corresponds to different relative concentration of free and bound NADH. Optical metabolic fingerprint of single cells are calculated by averaging the phasor coordinates over the segmented region of interest of the cells (red circular cursor). Cell phasor fingerprints are represented in the phasor scatterplot

by single points located along the metabolic trajectory between glycolysis and Oxidative Phosphorylation (OXPHOS). See also Figure S1.

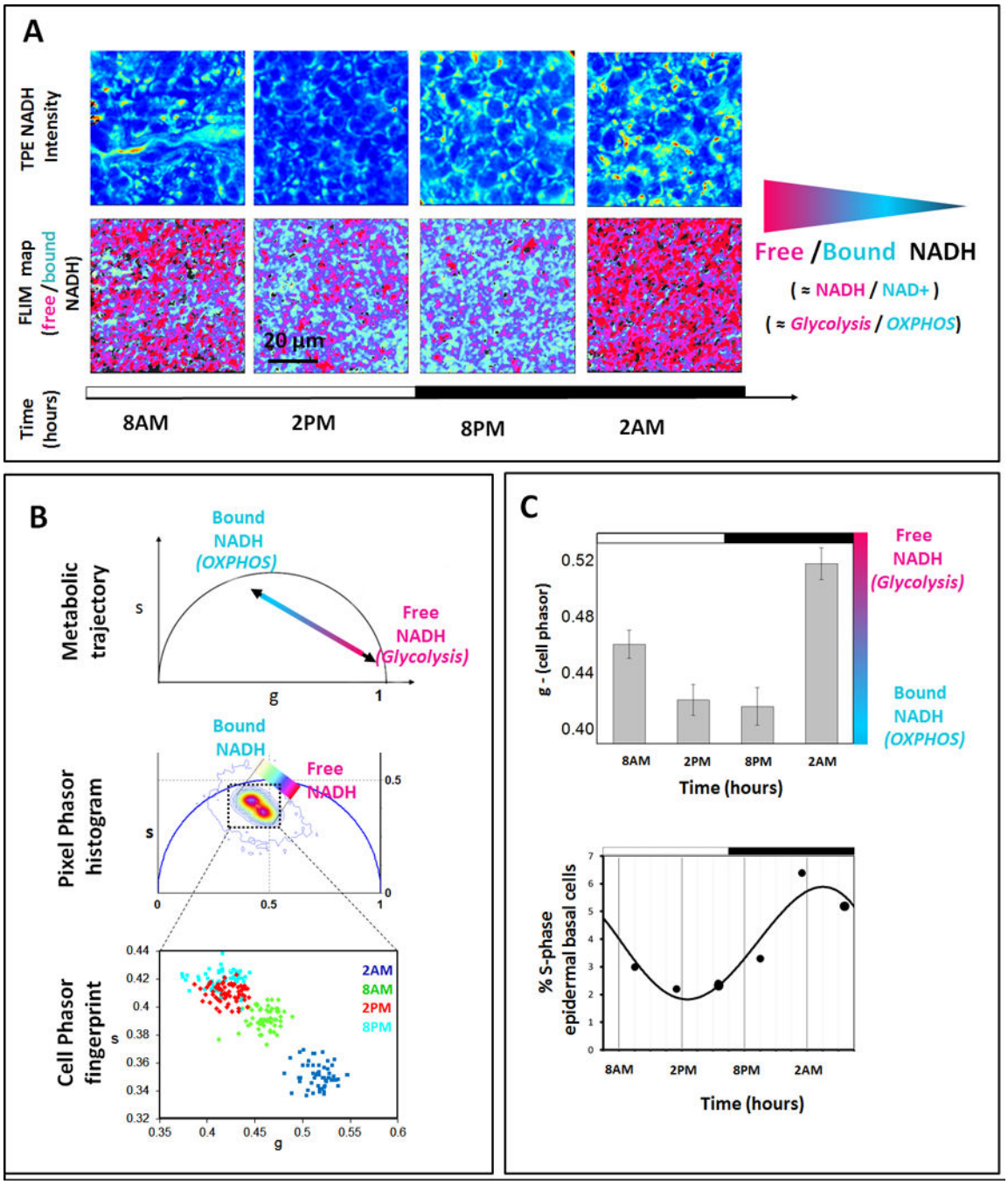

Figure 2. Free to bound NADH metabolic circadian oscillations in stem cells of the epidermis basal layer

(A) TPE fluorescence intensity *in vivo* images of stem cells within the epidermis basal layer excited at 740 nm with respective FLIM color maps at 740 nm of the relative concentrations of free NADH and bound NADH. Red-purple color indicates a high free/bound NADH ratio, while violet, cyan and white indicate linearly and progressively decreasing free/bound NADH ratios. Different ratios of free and protein-bound NADH reflect different redox ratios (NADH/NAD+) and rates of glycolysis and oxidative phosphorylation (**B**) Different relative

concentrations of free and Bound NADH correspond to a metabolic trajectory in the phasor plot between Glycolysis and OXPHOS, respectively. The linear cluster in the pixel Phasor histogram represents all possible relative concentrations of free NADH (purple) and bound NADH (white). Scatter plot of the cell phasor of all stem cells optical metabolic fingerprint at different times of the day: 2 AM (blue), 8 AM (green), 2 PM (red) and 8 PM (cyan). (**C**) The top shows a histogram of the g coordinate of the cell phasor fingerprint (which is proportional to the free/bound NADH ratio) displaying a circadian metabolic oscillation. All distributions are statistically different (t-rest $p<0.0001$). The bottom shows the average number of stem cells in S-phase over 24 hours as determined by BrdU incorporation (Geyfman, 2012). See also Figure S2.

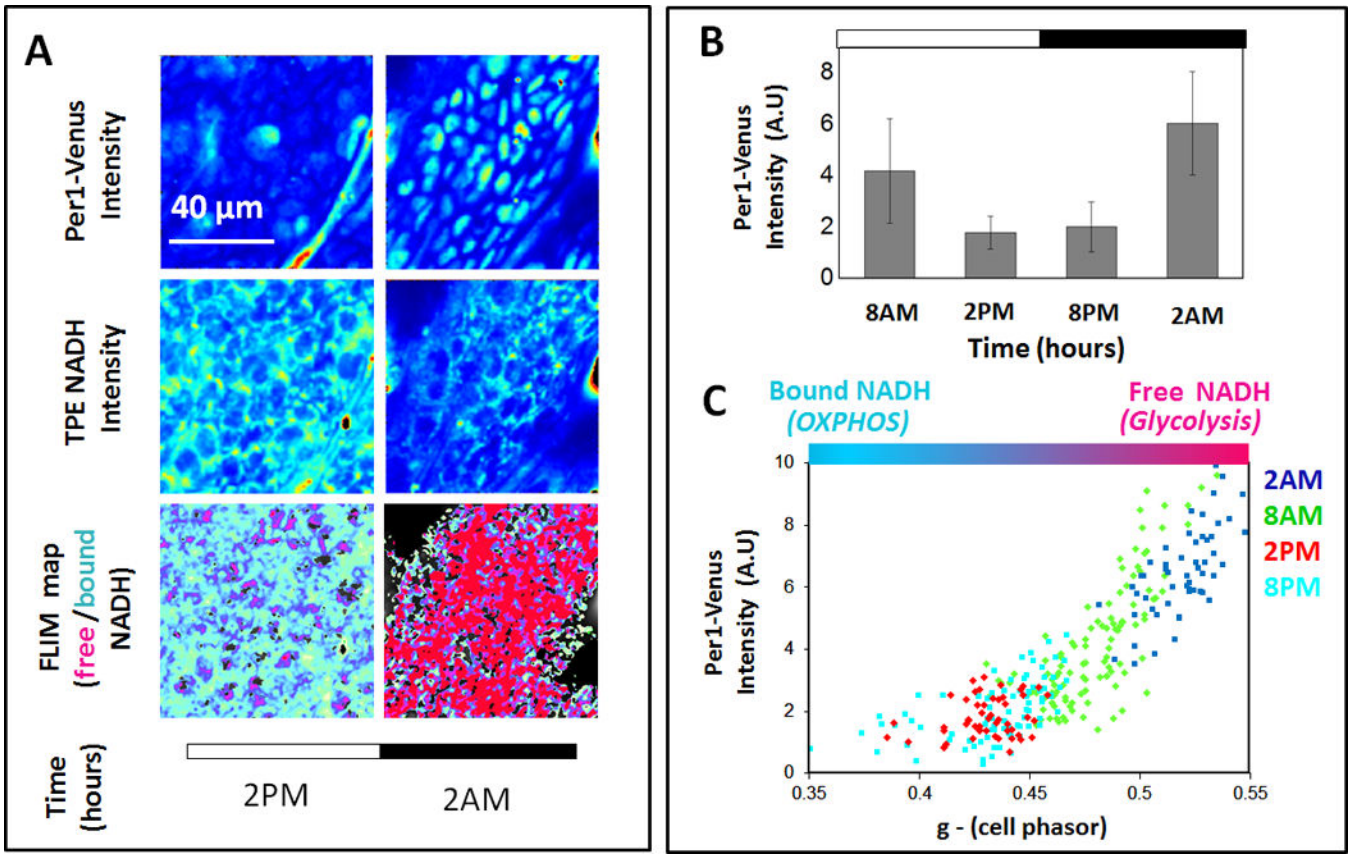

Figure 3. Metabolic cell heterogeneity in epidermal stem cells correlates with the clock phase

(A) TPE *in vivo* images of the epidermis basal cell layer expressing Per1-Venus reporter after excitation of stem cells at 940 nm. For the same field of view TPE intensity images of NADH and FLIM color maps at 740 nm of the relative concentrations of free NADH and bound NADH are represented. Red-purple color indicates a high free/bound NADH ratio, while violet, cyan and white indicate linearly and progressively decreasing free/bound NADH ratios. **(B)** Histogram of the average Per1-Venus Intensity from single stem cells display a circadian oscillation in phase with the oscillation of the g coordinate of cell phasor fingerprint (Fig.2). **(C)** Single stem cell Per1-Venus intensity displays a linear correlation with their metabolic fingerprint. See also Figure S3.

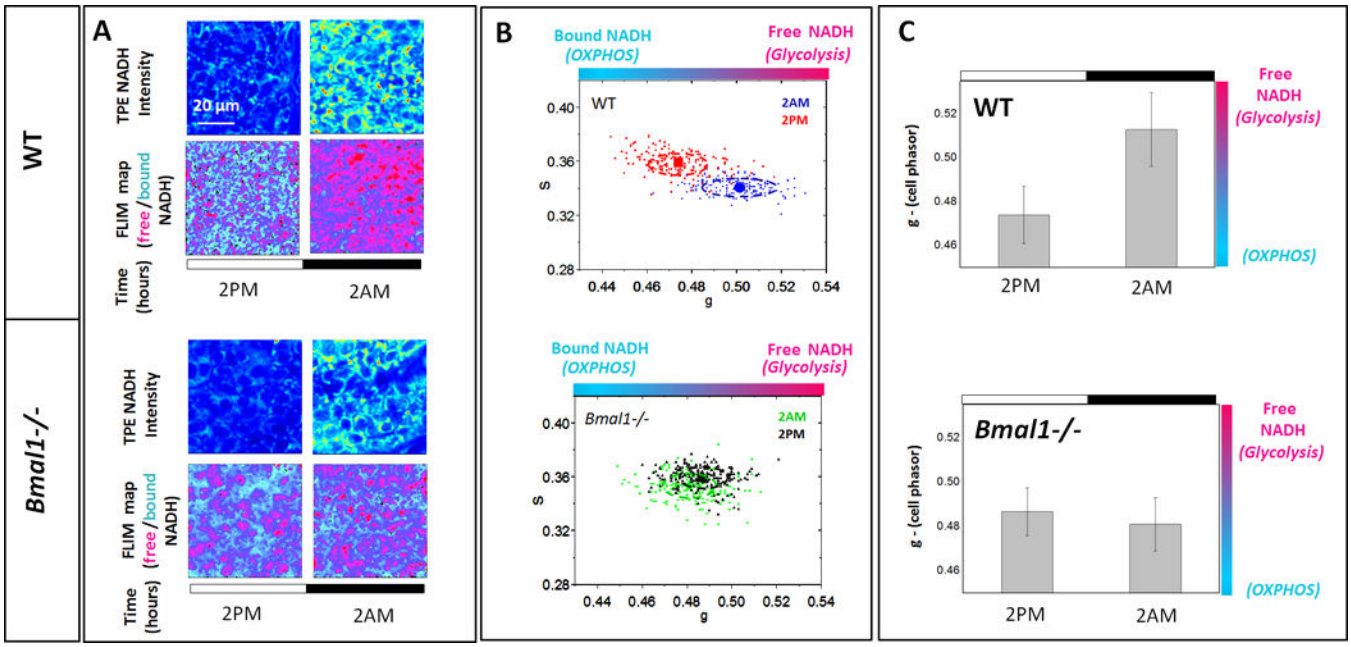

Figure 4. NADH metabolic oscillations are disrupted in the *Bmal1*−/− epidermal basal layer

(**A**) Two-photon fluorescence intensity *in vivo* images of stem cells within the epidermis basal cell layer of WT and *Bmal1*−/− mice excited at 740 nm at two different time points. Phasor FLIM color maps at 740 nm of the relative concentrations of free NADH and bound NADH. Red-purple color indicates a high free/bound NADH ratio, while violet, cyan and white indicate linearly and progressively decreasing ratios free/bound NADH ratio. (**B**) Scatter plot of the cell phasor of all stem cells optical metabolic fingerprint at different time of the day: 2 AM (blue), 2PM (red) measured in WT mice (t-test $p<0.0001$), and 2 AM (green), 2PM (black) measured in *Bmal1*−/− mice (t-test $p=0.37$). (C) The circadian metabolic oscillation of the cell phasor fingerprint g coordinate (proportional to the free/bound NADH ratio) is disrupted in *Bmal1*−/− mice. See also Figure S4.